# Evaluation of Seismic Behavior of a Braced Tubular Steel Structure by Pseudodynamic Testing

P. B. Shing
A. S. Javadian-Gilani
S. A. Mahin

Department of Civil Engineering,
University of California,
Berkeley, Calif. 94720

*The inelastic seismic behavior of an X-braced, tubular steel frame is studied experimentally by means of pseudodynamic testing. The pseudodynamic method, which utilizes a numerical algorithm in the on-line computer control of a test specimen, can realistically simulate the seismic response of a structural model. This paper presents a brief outline of the experimental procedure and the results of the tubular frame tests, including the global responses, the inelastic energy-dissipation capabilities, and the failure mechanism of the frame at various excitation levels. Correlation of these results with previous experimental studies illustrates the feasibility and accuracy of the new test method.*

## Introduction

To exploit limited oil resources, many offshore drilling towers are constructed in seismically active areas, such as the coastal regions of Southern California. To reduce construction costs while maintaining conservative safety precautions, the American Petroleum Institute (API) design criteria [1] permit inelastic deformations of structural members during severe earthquake excitations. However, the API provisions specify that the structures should remain stable and develop high energy-absorption capabilities under extreme seismic conditions. Experimental studies regarding the inelastic behavior of such structures provide valuable information for assessing design criteria and for improving current analytical techniques. Recently, an on-line computer-control (pseudodynamic) method has been developed to simulate quasi-statically the inelastic dynamic response of structures to seismic excitations.

The pseudodynamic method retains the economy and versatility of conventional quasi-static testing. Moreover, it produces results as informative as those of shaking table tests by accounting for the changing dynamic characteristics of a test structure. This experimental technique was initiated at the University of Tokyo in Japan, where it was successfully applied to the testing of building systems and components [2-4]. Analytical verifications of the method were performed at the University of Michigan, Ann Arbor [5] and the University of California, Berkeley [6]. The pseudodynamic testing facilities implemented at the Structural Engineering Laboratory at Berkeley were recently used to test the seismic behavior of a tubular steel frame, which was a 5/48-scale planar model of a representative X-braced offshore tower designed according to API wave and earthquake criteria. In this paper, we present the results of these tests, as well as a brief outline of the experimental procedure.

Tests were performed sequentially with increasing magnitude of earthquake excitations, corresponding to API "strength" and "ductility" level earthquakes as well as to a "Maximum Credible" event. This experimental program was intended to reproduce the results of shaking table tests performed by Ghanaat and Clough [7] on a similar structure. Larger scale frame models of similar design were also tested quasi-statically by Zayas, et al. [8]. The results of these three experimental programs are compared here to verify the reliability of the pseudodynamic test method and to study the inelastic frame behavior under various experimental conditions. Furthermore, based on these results, design implications and future experimental research needs are discussed.

## Pseudodynamic Test Method

**Theoretical Basis.** The equations of motion of a discretized structural system can be expressed in terms of a family of second-order differential equations. With the knowledge of the mass, damping, and stiffness properties of a system, the governing equations of motion can be numerically solved by a direct step-by-step integration method for any arbitrary external excitations. This is a well-established numerical procedure in structural dynamics; and the mass, damping, and stifffness matrices of a discretized system can be formulated by the finite element method [9, 10]. In pseudodynamic testing, the dynamic behavior of a structure is experimentally simulated, using the same numerical approach. However, instead of obtaining the stiffness matrix by finite element formulation, the restoring forces developed by structural deformations are directly measured from the test specimen during an experiment. Due to this fact, the inelastic dynamic response of a structure can be accurately simulated

Contributed by the Offshore Mechanics Committee of the Petroleum Division and presented at the 3rd International Symposium on Offshore Mechanics and Arctic Engineering, ETCE, New Orleans, Louisana, February 12-16, 1984, of THE AMERICAN SOCIETY OF MECHANICAL ENGINEERS. Manuscript received by the Petroleum Division, June 22, 1983; revised manuscript received January 6, 1984.

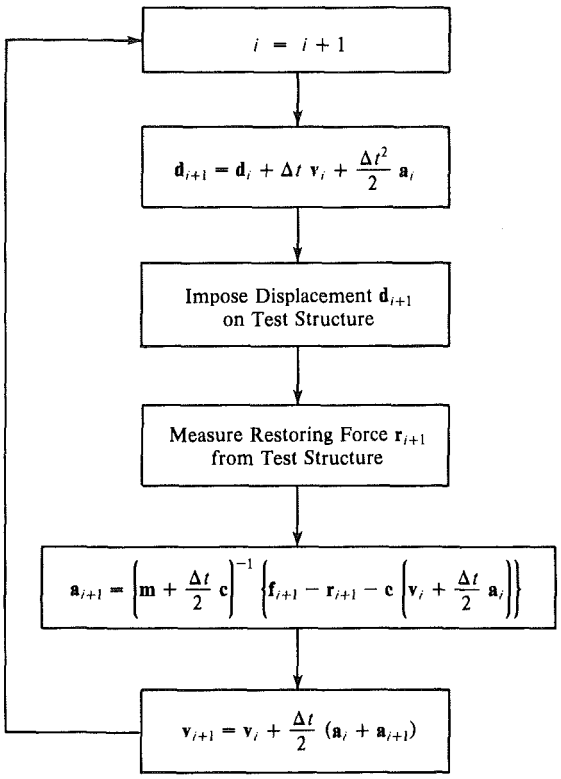


**Fig. 1 Newmark explicit algorithm in pseudodynamic testing**

in a laboratory, without the uncertainties associated with idealized inelastic mechanical properties of the structure.

**Numerical Formulation.** Considering the dynamic response of a multiple-degree-of-freedom structure to an excitation of duration $T$, which is subdivided into $N$ equal intervals $\Delta t$, i.e., $\Delta t = T/N$, we can write the equations of motion at time $(i+1)\Delta t$ as

$$\mathbf{m}\,\mathbf{a}_{i+1} + \mathbf{c}\,\mathbf{v}_{i+1} + \mathbf{k}\,\mathbf{d}_{i+1} = \mathbf{f}_{i+1} \tag{1}$$

where $\mathbf{m}$, $\mathbf{c}$, and $\mathbf{k}$ are the mass, damping, and stiffness matrices of the structure; $\mathbf{a}_{i+1}$, $\mathbf{v}_{i+1}$, and $\mathbf{d}_{i+1}$ are the acceleration, velocity, and displacement vectors at $(i+1)\Delta t$; and $\mathbf{f}_{i+1}$ is the external force excitation vector. By considering equation (1) at $i = 0, 1, 2, \ldots, N$, an approximate numerical solution of the equations of motion can be evaluated at these time steps using a step-by-step integration method. Different step-by-step integration methods are available [10]. We adopt the definition that an integration method is explicit if displacement $\mathbf{d}_i$ is assumed to be dependent on $\mathbf{d}_k$, $\mathbf{v}_k$, and/or $\mathbf{a}_k$, for $k < i$. For $k \leq i$, the method is implicit.

To solve the equations of motion during a pseudodynamic test, we can use an explict form of the Newmark integration method [11], which assumes that

$$\mathbf{v}_{i+1} = \mathbf{v}_i + \frac{\Delta t}{2}(\mathbf{a}_i + \mathbf{a}_{i+1}) \tag{2}$$

$$\mathbf{d}_{i+1} = \mathbf{d}_i + \Delta t \mathbf{v}_i + \frac{\Delta t^2}{2}\mathbf{a}_i \tag{3}$$

By substituting $\mathbf{v}_{i+1}$ in equation (1) with equation (2), we can solve for $\mathbf{a}_{i+1}$ in terms of $\mathbf{v}_i$, $\mathbf{a}_i$, and $\mathbf{k}\,\mathbf{d}_{i+1}$. Since the product $\mathbf{k}\,\mathbf{d}_i$ can be measured as the restoring-force vector $\mathbf{r}_i$ in every step of a test, the displacement response $\mathbf{d}_{i+1}$ can be readily computed by using the Newmark algorithm, and imposed on a test structure, as shown in Fig. 1. The mass matrix $\mathbf{m}$ and viscous damping $\mathbf{c}$ have to be analytically modeled. In general, a lumped-mass matrix can be accurately assumed for a structure which has most of its mass concentrated at defined degrees of freedom.

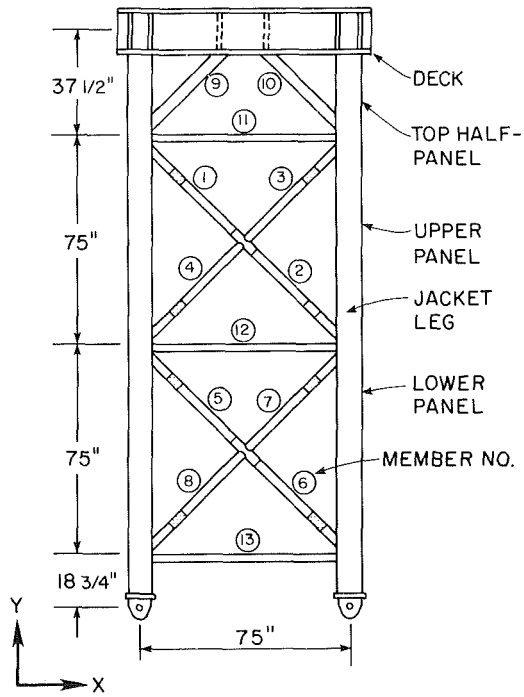


**Fig. 2 Frame configuration and member numbering (1 in. = 25.4 mm)**

**Reliability.** Although the Newmark integration method yields an approximate solution, numerical errors are negligible when a sufficiently small integration step $\Delta t$ is used. The method is stable (i.e., solution will not grow without bound for any arbitrary initial conditions) when $\omega_M \Delta t \leq 2$, where $\omega_M$ is the highest angular frequency of a structure. In general, to obtain an accurate vibration response at frequency $\omega$, $\omega\Delta t$ should not be greater than 0.5.

Since pseudodynamic response is simulated at a prolonged time scale, the strain-rate effect may influence the inelastic structural behavior. However, previous studies show that this is insignificant for steel structures as long as the strain rate is limited by the frequency range of ordinary structures [12].

The most significant causes of inaccuracy in pseudodynamic testing are experimental errors. Since the displacement response computed at each step of a test is dependent on the experimental feedback at the previous step, feedback errors have a cumulative effect. This error-propagation phenomenon has been investigated in a previous study [6], which indicates that errors of systematic nature can induce significant energy effects in a pseudodynamic simulation. These errors result mainly from improper instrumentation and test apparatus. Nevertheless, error checking procedures and numerical correction methods are available to achieve reliable test results.

## Experimental Program

**Features of Test Frame.** For correlation purpose, the frame selected for pseudodynamic testing had the same design as the one tested on a shaking table [7]. The geometric configurations and member size specifications of the two frames were identical. The 17 ft 9 1/8 in. (5.4 m) high and 75 in. (1.9 m) wide tubular frame consisted of three braced panels (see Fig. 2). It represented a complete bent of a 5/48 scale model of a Southern California platform designed according to API wave and earthquake criteria. The operation deck was simulated by a stiff beam. During the shaking table tests, a 40.4-kip (179.8 kN) dead load, which accounted for 99 percent of the total frame weight, was superimposed on the top of the frame to represent the weight of deck appurtenances. The same mass distribution was assumed in the pseudodynamic tests.

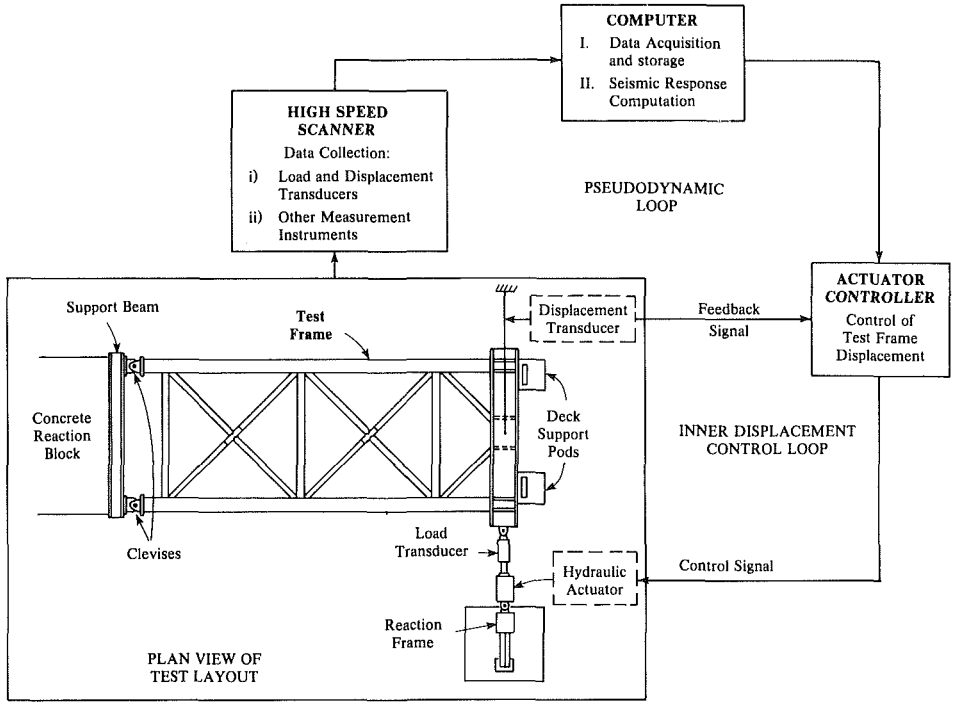


**Fig. 3 Schematic of pseudodynamic test setup**

**Table 1 Member sizes and material properties**

| Member no. or description | Tube dimensions nominal diameter ($D$) × wall thickness ($t$) (in.) | Yield stress (ksi) | Ultimate stress (ksi) |
|---|---|---|---|
| 1,3 | 2 1/2 × 0.049 | 30.7 | 40.2 |
| 2,4 | 2 1/2 × 0.049 | 27.4 | 37.8 |
| 5,6,7,8 | 3 × 0.083 | 31.5 | 51.7 |
| 9,10 | 3 1/2 × 0.083 | 32.0 | 53.0 |
| 11,12,13 | 2 1/2 × 0.049 | 19.6 | 41.0 |
| Jacket legs | 8 × 0.188 | 48.0 | 62.2 |

The section sizes of the frame members are listed in Table 1, with member identification numbers shown in Fig. 2. The upper-panel diagonal braces had a $D/t$ (nominal diameter/wall thickness) ratio of 51; and that of the lower-panel braces was 36. All the braces were heat treated to obtain a yield stress similar to that of A36 steel. The average yield and ultimate stresses of the annealed materials, based on coupon tests, are shown in Table 1 as well. The variation of yield stresses in similar tubular sections was due to separate annealing processes. The frame was so designed that the failure mechanism would be dominated by the yielding and buckling of the diagonal braces. For this reason, the cross-joints of the braces were reinforced with thick-walled inserts to prevent premature joint failures.

**Pseudodynamic Formulation.** Since most of the mass was concentrated at the top of the frame, one could reasonably assume that the frame was a single-degree-of-freedom system in pseudodynamic testing. Moreover, the $P$-$\Delta$ effect of the dead load had to be numerically modeled because the frame was tested horizontally. With these considerations, the equation of motion of the test frame is

$$m\,a_{i+1} + c\,v_{i+1} + (k+k_g)\,d_{i+1} = f_{i+1} \tag{4}$$

which is a scalar form of equation (1). With the 40.4 kip (179.8 kN) dead load, the geometric stiffness $k_g$ (i.e., weight/height), which accounts for the $P$-$\Delta$ effect, was $-0.196$ kip/in. ($-34.3$ kN/m), and the mass $m$ was 0.105 kip sec$^2$/in. (18.3 m.t.). Viscous damping ratio was assumed to be 1.5 percent, which was an approximate value measured from the shaking table tests. For seismic excitations, $f_{i+1} = -m\,\ddot{a}_{i+1}$, where $\ddot{a}_{i+1}$ was the discretized ground acceleration at time $(i+1)\Delta t$.

Conseqently, by measuring the restoring force $r_{i+1} = k\,d_{i+1}$ directly from the test frame in each integration step, the displacement response could be solved from equation (4) and imposed on the frame in a stepwise manner, using the algorithm in Fig. 1.

**Test Setup and Instrumentation.** The pseudodynamic test setup is briefly described in Fig. 3. The frame base was attached to a stiff beam on a reaction block by clevises; and free horizontal movement was allowed at the frame top. A minicomputer was used for displacement computation, and for data acquisition and storage. The displacement increment computed at each step was transferred as a voltage signal to an actuator controller, which commanded a hydraulic actuator to impose the specified displacement on the test frame. The actuator was connected to the frame top (or deck) by a clevis; and the displacement control loop was completed by a displacement-feedback transducer measuring the center point displacement of the deck in line with the actuator. After the correct displacement was imposed on the frame, the restoring-force measured by a load transducer mounted on the actuator (as well as data from other measurement instruments) was collected and transferred to the computer by a high-speed scanner. The next displacement increment was, then, computed using the restoring-force feedback; and the whole process was repeated.

The yielding and buckling behavior of the diagonal braces was carefuly monitored by linear potentiometers and load transducers. The out-of-plane displacements of the cross-joints were also measured.

**Test Sequence.** The earthquake excitations used in the pseudodynamic tests were horizontal table accelerations recorded from the previous shaking table tests. They were derived from the Taft 1952 S69E earthquake record. Due to the filtering of high frequency components from the record used for the shaking table tests and the table-structure interaction phenomenon, the recorded accelerations differed slightly from the original Taft record. To obtain the dynamic

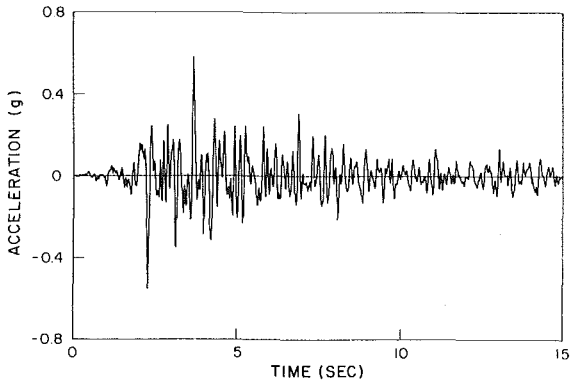


Fig. 4 Taft accelerogram (ductility level)

Table 2 Test sequence

| Test no. | Earthquake levels | Maximum ground acceleration ($g$) |
|---|---|---|
| 1 | Half-strength | 0.138 |
| 2 | Strength | 0.276 |
| 3 | Ductility | 0.581 |
| 4 | Half-strength | 0.138 |
| 5 | Max. credible | 1.228 |
| 6 | Max. credible | 1.228 |

similitude of the prototype, the time span of the acceleration record was scaled down by a factor of 0.48.

The test sequence is listed in Table 2. The magnitude of ground accelerations varied from 0.138$g$ to 1.228$g$. Tests 2 and 3 corresponded to the "strength" and "ductility" level earthquakes, respectively, according to the API criteria for seismic zone 4, while Tests 5 and 6 were extreme events. Tests 1 and 4 were half-"strength level" events used to study the change of dynamic behavior after significant structural damages. A typical Taft record is shown in Fig. 4.

## Verification Tests

As mentioned before, pseudodynamic tests are susceptible to experimental errors. To ensure the credibility of test results, some preliminary tests were carried out to check the accuracy of the experimental apparatus.

In pseudodynamically simulated free-vibration tests, excessive structural damping was detected because of the friction in the clevises and in the frame support apparatus. This friction was numerically removed from the restoring-force measurements. The corrected free-vibration responses are shown in Fig. 5($a$), with zero and 1.5 percent numerically specified viscous damping. The gradual decrease of displacement amplitudes in the zero damping case was caused by hysteretic energy dissipation related to localized yielding of the frame members due to residual stresses and stress concentrations. However, this was insignificant with respect to the 1.5 percent viscous damping. The natural period of the frame measured from the pseudodynamic free vibrations was 0.402 s, which indicated an elastic frame stiffness of 25.57 kip/in. (4480 kN/m). This was consistent with the stiffness measured from static tests, but lower than the analytically computed stiffness (which is 32.4 kip/in. or 5680 kN/m). This discrepancy can be explained by the measured base-support flexibility.

Finally, an elastic test was performed using a small magnitude Taft record (0.069$g$). An excellent correlation can be observed between the pseudodynamic and analytical results (see Fig. 5($b$)). Again, the test result had a little more damping due to local nonlinearities.

## Experimental Results

**Inelastic Seismic Response.** The global responses of the

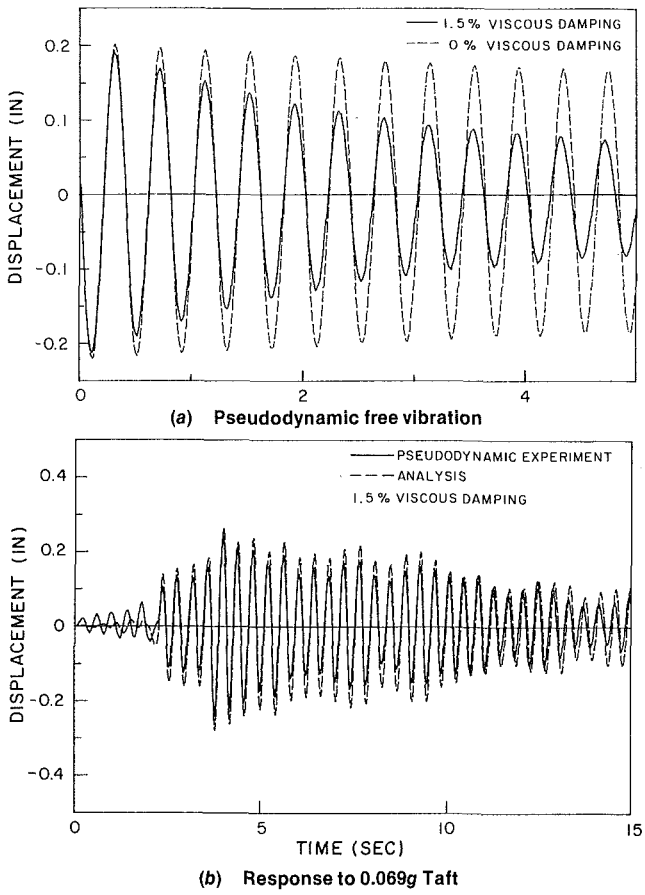


Fig. 5 Verification tests (1 in. = 25.4 mm)

frame in the six consecutive Taft events are shown by the deck-level displacement time histories and the hysteretic loops of lateral frame load versus deck displacement in Fig. 6. The change of response characteristics of the frame in each event, as observed from the figure, manifested the extent of structural damages developed. The most significant transitions of response characteristics appeared in the "ductility level" and the first "maximum credible" events as residual displacements and period elongations in the displacement time histories, which were accompanied by significant hysteretic energy dissipations. These corresponded to the first occurrence of severe yielding and buckling of the diagonal braces in the upper and lower panels, respectively. The load resistance and inelastic energy-dissipation capabilities of the frame were mainly offered by the diagonal braces. At the final stage, the upper-panel braces ruptured; and the frame lost more than 50 percent of its lateral stiffness but retained a good energy-dissipation capability.

The seismic behavior of the frame during the six events are briefly summarized in the followings:

(*i*) *Half-"Strength Level" Event.* During the half-"Strength-Level" excitations, the frame experienced a maximum deck-level displacement and lateral load of 0.5 in. (12.7 mm) and 12.5 kips (55.6 kN), respectively, at about 3.8 s of the 15-s record (Fig. 6($a$)). A small non-linearity was observed in the lateral load versus deck displacement curves. This was attributed to localized yielding in the braces. The most significant localized yielding was observed in brace 2.

(*ii*) *"Strength Level" Event.* During the "Strength Level" excitations, the maximum deck displacement and lateral load experienced by the frame were 0.8 in. (20.3 mm) and 18 kips (80.1 kN), respectively, (Fig. 6($b$)). Considerable energy dissipation was observed in the frame hysteretic loops.

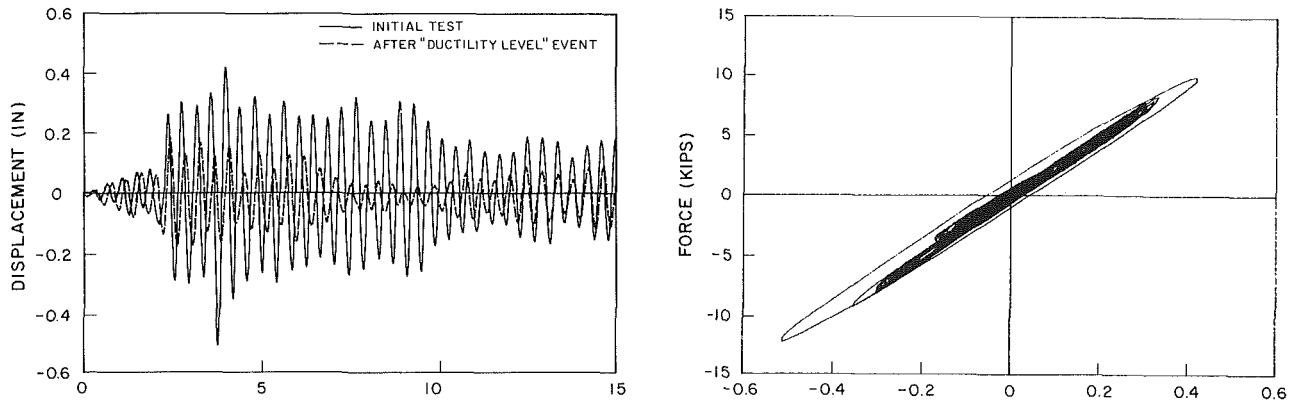


(a) Half-"strength level"

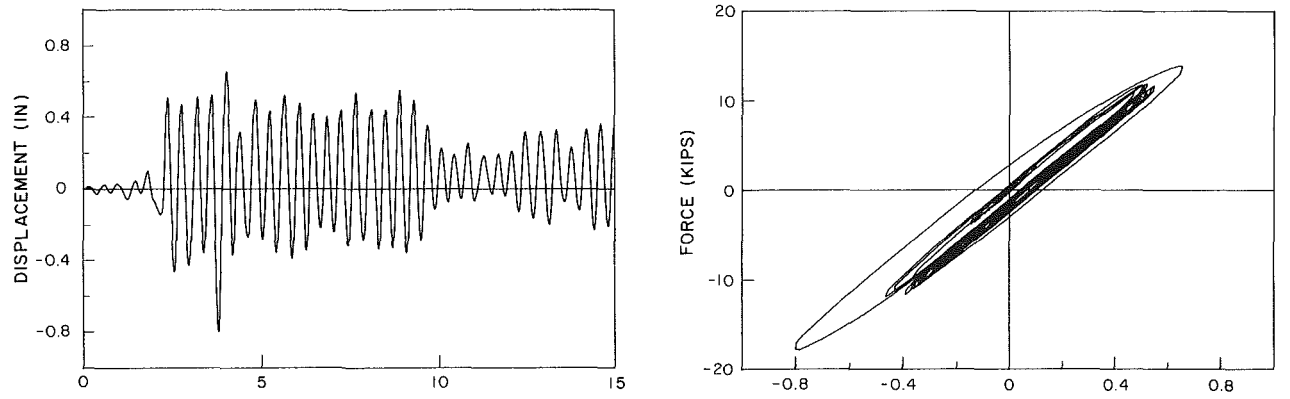


(b) "Strength level"

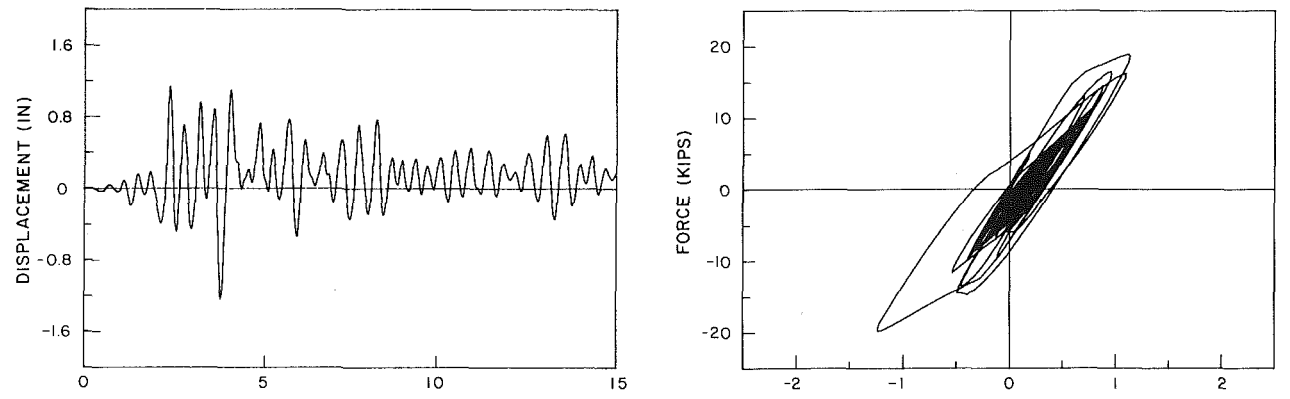


(c) "Ductility level"

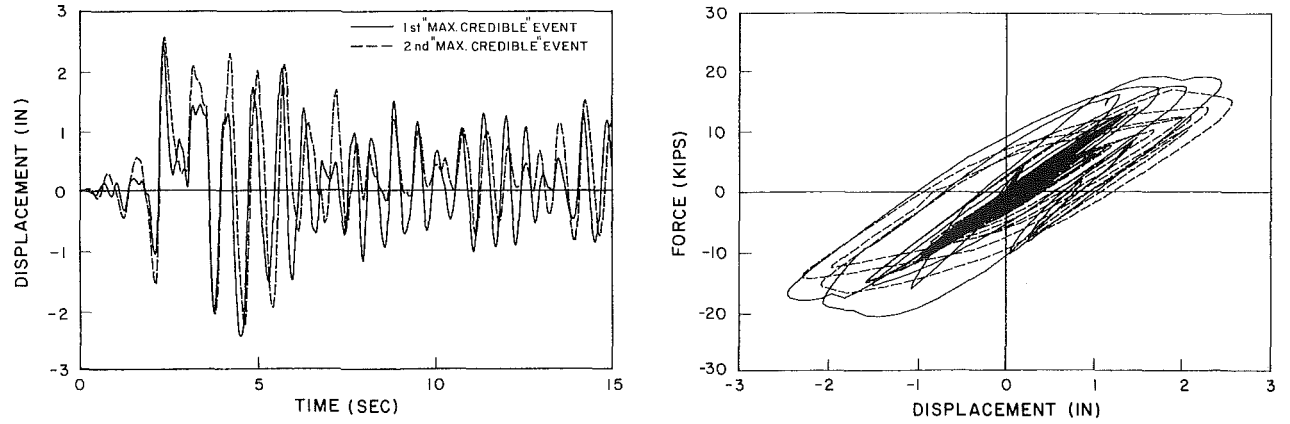


(d) "Maximum credible"

**Fig. 6 Pseudodynamic test results (1 in. = 25.4 mm, 1 kip = 4.45 kN)**

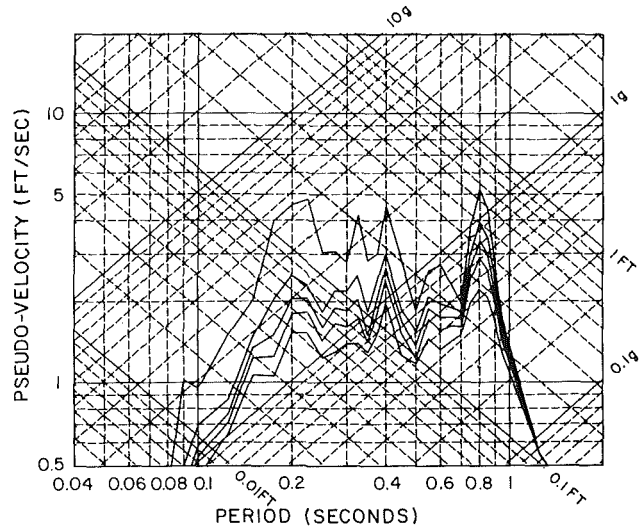


Fig. 7 Response spectra of Taft 0.581g (reference [7]) (1 ft = 0.3 m)

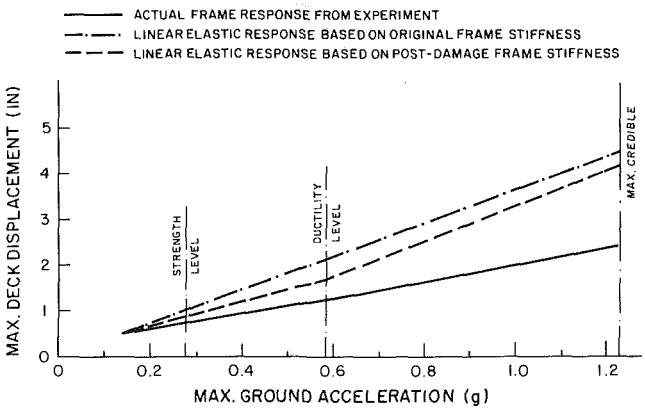


Fig. 8 Maximum frame response (1 in. = 25.4 mm)

All the diagonal braces showed limited local nonlinearities except braces 2 and 4, which had pronounced tensile and compressive yielding. This was in part due to a lower yield stress of the material for braces 2 and 4 (Table 1). At the end of the test, a small residual displacement was observed; the frame stiffness was reduced to 24.6 kip/in. (4310 kN/m).

(*iii*) *"Ductility Level" Event.* The frame reached a peak displacement of 1.2 in. (30.5 mm) and a maximum load of 20 kips (89 kN) (Fig. 6(*c*)) during the "ductility level" earthquake. The relatively small increase of lateral frame load was due to the development of significant frame nonlinearity. Sudden reductions of frame stiffness occurred at large displacement levels, as shown by the frame hysteretic loops in Fig 6(*c*). These corresponded to the compressive buckling and tensile yielding of braces 2 and 4. The buckling strengths of these braces deteriorated rapidly to about 1/3 of their original values during later displacement cycles. Tensile strength was also drastically reduced due to brace tearing in local buckling regions. Braces 1 and 3 remained essentially elastic throughout the test, while only localized yielding occurred at the lower-panel diagonal braces. After the test, the elastic frame stiffness measured was 23.6 kip/in. (4130 kN/m).

(*iv*) *Post-Damage Half-"Strength Level" Event.* The displacement response of the frame in this test was much smaller than that in the initial half-"Strength Level" event. The peak displacement was 0.18 in. (4.6 mm) (Fig. 6(*a*)).

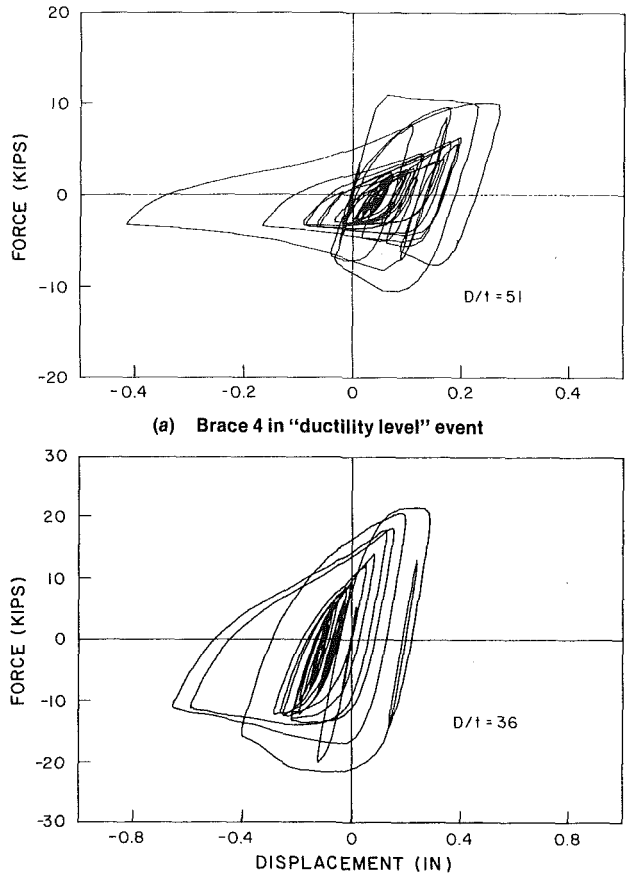


Fig. 9 Brace hysteretic loops (1 in. = 25.4 mm, 1 kip = 4.45 kN)

Period elongation was observed in the displacement history, indicating a reduced frame stiffness.

(*v*) *"Maximum Credible" Event.* During the "maximum credible" event, the peak displacement of the frame was 2.4 in. (61 mm) (Fig. 6(*d*)). The latetral load reached a maximum frame capacity of 21 kips (93.5 kN). Braces 2 and 4 ruptured, passing the lateral load resistance completely to the lower-panel diagonal braces by means of the jackets. However, the frame hysteretic loops showed stable energy dissipation throughout the test. Buckling occurred in all the four lower-panel diagonal braces, but braces 5 and 7 exhibited twice as much axial deformations as braces 6 and 8. After the test, the frame stiffness deteriorated to 11.74 kip/in. (2060 kN/m) (i.e., 46 percent of the original value).

(*vi*) *Second "Maximum Credible" Event.* During the second "maximum credible" event, the displacement response of the frame was similar to the previous one except that some additional period elongation was observed. Severe tensile yielding and compressive buckling were developed in braces 5 and 7, while braces 6 and 8 had relatively limited inelastic deformations. The buckling strengths of braces 5 and 7 were reduced by about 50 percent at later displacement cycles. The final stiffness of the frame was 10.41 kip/in. (1820 kN/m). The energy-dissipation capability of the frame deteriorated slightly as shown by the hysteretic loops in Fig. 6(*d*).

**Effect of Structural Damage on Seismic Response.** As shown by the response spectra of a Taft event in Fig. 7, the peak elastic response of a structure to the excitation record can vary within a considerable range, depending on its natural frequency and viscous damping. For the elastic responses in Fig. 6(*a*), the tower initially had a period of about 0.4 s corresponding to a peak in the response spectra. Lengthening

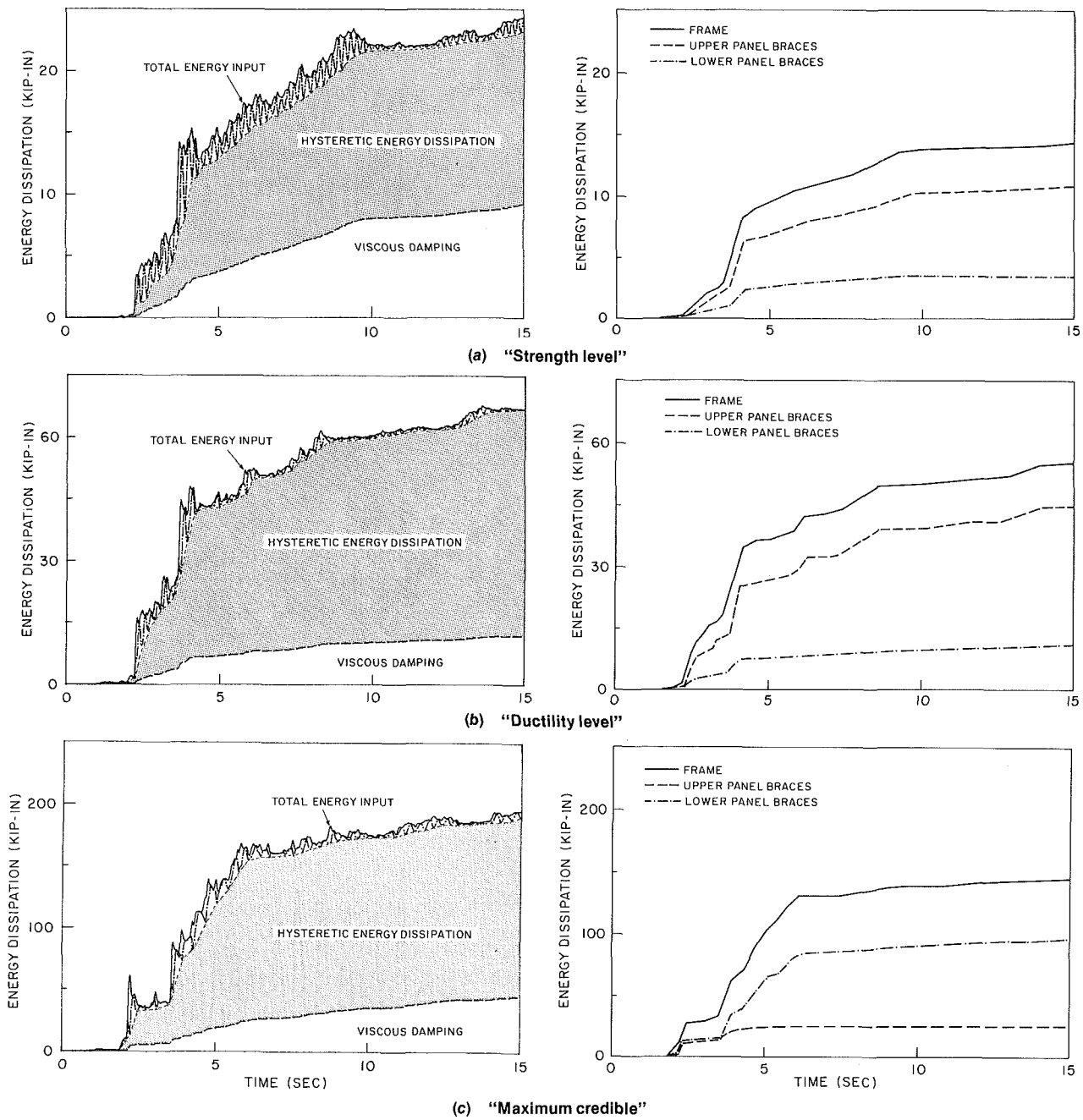


**Fig. 10 Energy dissipation in the frame responses (1 kip-in. = 0.113 kN·m)**

the period due to damages in the "strength" and "ductility" level events moved the period into a spectral valley, thereby reducing the response considerably. This trend depends on the period shift, but also on the particular record used.

The response of a damaged structure is usually different from that of an original one because of stiffness degradation and hysteretic energy dissipation. In Fig. 8, we compare the peak elastic displacement responses of the frame based on the original and post-damage frame stiffness, respectively, at each excitation level. These values were obtained from the elastic spectrum in Fig. 7, assuming 1.5 percent damping. The significance of effective hysteretic damping can be realized from the experimental data curve plotted in the same figure. The curve shows that the actual peak displacement response of the frame was about 60 percent of the spectral prediction during the "maximum credible" event due to hysteretic damping. Therefore, inelastic structural deformation is desirable during intense seismic excitations, as long as the structure remains stable and develops a good energy-dissipation capability.

**Inelastic Brace Behavior.** Lateral buckling of the load resisting braces concentrated mainly at one of the braces along a full diagonal; and the out-of-plane displacements of the cross-joints remained relatively small. The upper-panel braces, which had a smaller cross-sectional area and a larger $D/t$ ratio than the lower-panel ones, buckled first. Their buckling strength deteriorated rapidly with cycling until the final rupture. The stability and the energy-dissipation capability of the frame during the "maximum credible" events were mainly contributed by the stronger and stockier lower-panel braces.

The hysteretic loops of axial force versus axial displacement of braces 4 and 7 are shown in Fig. 9. It is apparent that the stockier brace 7 had more efficient energy-dissipation hysteretic loops than brace 4, as well as a lower rate of

strength deterioration. The rapid deterioration of tensile and compressive resistance of brace 4 that occurred during the "ductility level" event was caused by local buckling, which was responsible for tearing and final rupture of the brace. Brace 7 was more resistant to local buckling due to its smaller $D/t$ ratio.

**Energy Dissipation.** The energy dissipation in the frame responses during the three major events is illustrated in Fig. 10, which shows that most of the input energy from the ground motions was dissipated in the form of hysteretic damping. The viscous damping effect was relatively small when compared with the hysteretic energy dissipation, especially for the higher level events. The maximum amount of energy absorption in a single monotonic displacement occurred at about 3.8 s during each event, coinciding with the peak acceleration of the Taft record (Fig 4). The amount of energy absorbed during this the maximum excursion was about 7 kip-in. (0.79 kN-m) in the "strength level" event, and about 31 kip-in. (3.5 kN-m) in the "maximum credible" case. These energy-absorption trends satisfy the API "ductility level" design criterion [1], which recommends that a structure should be capable of absorbing at least 4 times the amount of energy requried by the "Strength Level" criterion. Much of the absorbed energy was dissipated by inelastic deformations.

From Fig. 10, it is also apparent that the diagonal braces were responsible for nearly all the energy dissipation in the framed responses. During the "strength" and "ductility" level events, the inelastic deformations of the upper-panel braces contributed to most of the frame energy dissipation. In the "maximum credible" event, the upper-panel braces ruptured, and the lower-panel ones took over the energy-dissipation mechanism. The total amount of energy dissipated by the upper-panel braces in the three events was smaller than that by the lower-panel braces. Nevertheless, the upper-panel braces ruptured, while the lower-panel ones remained stable. This is in part due to the smaller $D/t$ ratio, as well as to the more evenly distributed inelastic deformations, of the lower-panel diagonal braces.

## Correlation With Previous Experimental Results

**Shaking Table Tests.** The comparison of pseudodynamic test results with those of shaking table tests [7] verifies the reliability of the pseudodynamic approach. Although a perfect correlation does not exist between the two experimental results, the inelastic seismic behaviors are similar and the failure modes of the two frames are identical. The most significant difference between the pseudodynamic and shaking table test specimens was in the lateral frame stiffnesses. The initial elastic stiffness of the shaking table test frame, computed from the period measured in a small level test, was 31 percent lower than the pseudodynamic frame's stiffness, and was considerably smaller than that predicted by analysis. Since the test frames were fabricated from brace members of identical size specifications, the stiffness discrepancy was apparently caused by the flexibility of the base supports as well as the significant table-structure interaction (rocking) observed during the shaking table tests. Due to the different stiffnesses, the pseudodynamic and shaking table frames had initial periods of 0.40 and 0.48 s, respectively. This led to very different linear elastic responses in accordance with the response spectra in Fig. 7 and as shown in Fig. 11(*a*). In addition, it was not possible to obtain an exact material match so that the yield stress of the upper-panel braces in the pseudodynamic specimen was about 7 ksi (48.2 MPa) greater than that in the shaking table frame. Consequently, a precise correlation of pseudodynamic and shaking table results would not be possible.

In spite of these, it is useful to compare the stiffness degradation, maximum deck displacements, and maximum

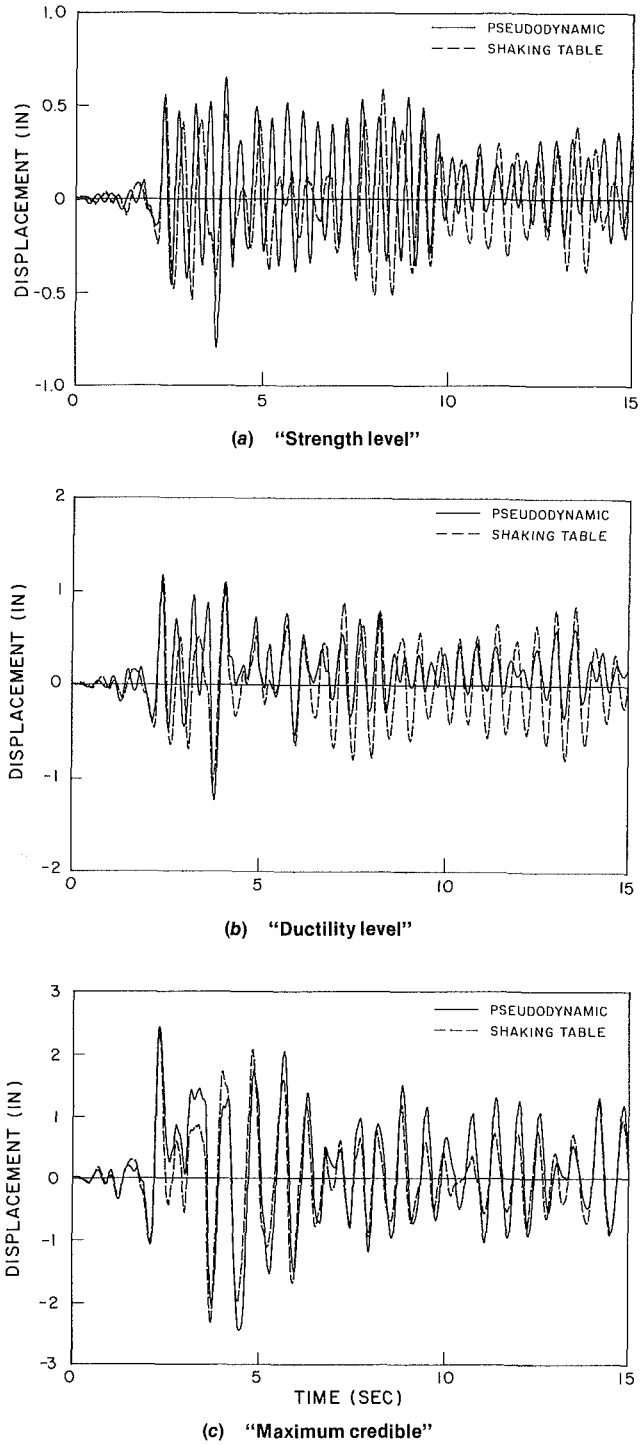


(*a*) "Strength level"

(*b*) "Ductility level"

(*c*) "Maximum credible"

**Fig. 11 Comparison of pesudodynamic and shaking table test results (1 in. = 25.4 mm)**

lateral loads experienced by the frames during the two separate experiments. These are listed in Table 3 and the displacements histories in the three major events of both experiments are compared in Fig. 11.

(*i*) *"Strength Level" Event.* Figure 11(*a*) shows that the displacement histories obtained from the "strength level" events of the two experiments are significantly different. However, the peak displacement values are in agreement with the response spectra in Fig. 7. Due to the greater deck displacement and the less flexible based support, the maximum lateral load experienced by the frame in the pseudodynamic test was twice as much as that in the shaking

**Table 3 Comparison of experimental results**

| Event levels | Pseudodynamic tests | | | Shaking table tests | | |
|---|---|---|---|---|---|---|
| | Stiffness (kip/in.) | Max. displ. (in.) | Max. load (kip) | Stiffness (kip/in.) | Max. displ. (in.) | Max. load (kip) |
| Strength | 24.6 | 0.8 | 18.0 | 17.4 | 0.6 | 9.5 |
| ductility | 23.6 | 1.2 | 20.0 | 15.3 | 1.2 | 16.1 |
| 1st max. cred. | 11.4 | 2.4 | 21.0 | 11.2 | 2.4 | 28.5 |

table test. This led to considerable yielding of the upper-panel braces in the pseudodynamic experiment, but only localized yielding occurred in the shaking table specimen.

(*ii*) *"Ductility Level" Event.* The displacement histories in the "ductility level" events (Fig. 11(*b*)) show better correlation than those in the previous case. The peak displacements are very close. This is attributed to the considerable amount of energy dissipation in the pseudodynamic test, during which severe yielding and buckling of the upper-panel braces occurred. On the other hand, only relatively moderate yielding of the upper-panel braces occurred in the shaking table test specimen.

(*iii*) *"Maximum Credible" Event.* Due to the rapid deterioration of the pseudodynamic frame's stifffness during the "maximum credible" event, its overall stiffness aproached that of the shaking table specimen (Table 3). Thus, the displacement responses of the two frames are very similar, as shown by Fig. 11(*c*). During this event, the upper-panel braces of the shaking table specimen buckled severely, while those of the pseudodynamic specimen ruptured. The final rupture of the braces in the former did not occur until the second "maximum credible" event. This shows that the shaking table specimen retained a greater load resistance than the pseudodynamic specimen. However, both frames retained good energy-dissipation capabilities.

The discrepancy between the experimental results is reasonable if the different dynamic characteristics of the two frames are taken into account. The more severe damage on the pseudodynamic frame is mainly due to its less flexible base support, which induced greater seismic loading on the test frame. Since the exact characteristics of the table-structure interaction are not clear, it can be difficult to obtain good correlations between analytical and shaking table test results. On the other hand, the base conditions of a pseudodynamic specimen can be easily modeled from the measured support flexibility. An excellent correlation has been observed between the elastic pseudodynamic response and an analytical simulation (Fig. 5(*b*)). Currently, substantial efforts are being extended to correlate analytical predictions with the inelastic pseudodynamic frame responses.

**Quasi-Static Tests.** The pseudodynamic test specimen was a 5/8-scale model of a frame previously tested by the conventional quasi-static method [8]. All the brace members of the pseudodynamic frame were appropriately scaled, such that the diagonal brace members of the two frames had very close $D/t$ ratios. Therefore, the failure modes of the two frames were very similar.

In the quasi-static test, 18 cycles of predetermined displacements were imposed on the frame with gradually increasing amplitudes. At displacement ductility levels comparable to those in the "strength level," "ductility level," and "maximum credible" events in the pseudodynamic testing, the stiffness of the quasi-statically tested frame deteriorated to 97, 79, and 57 percent of its original value, respectively. At each stage, brace damages were less severe than those in the pseudodynamic tests. This was due to the larger number of displacement cycles experienced by the pseudodynamic test frame, and consequently, the greater deterioration of the braces. Therefore, the inelastic displacement history experienced by a frame has a significant influence on its seismic performance. Since the conventional quasi-static approach neglects the dynamic characteristics of a sttucture, it is difficult to use these test results in assessing the potential seismic performance of a structure.

## Conclusions

The results of the tubular frame tests presented in this paper indicate the feasibility of the pseudodynamic method as an economical and reliable experimental technique to study the inelastic seismic behavior of structural systems. Based on these results as well as those from the previous experiments, the following conclusions can be obtained:

1 The pseudodynamic method accounts for the dynamic characteristics of a test structure, so that the realism of the test results is comparable to that of shaking table results. The implementation of the pseudodynamic testing facilities requires little more effort than the conventional quasi-static approach, i.e., on-line computer control software must be developed.

2 The pseudodynamic method provides well-controlled experimental conditions. The problem of table-structure interaction which may occur in shaking table testing does not exist in pseudodynamic tests. In addition, the size and weight of a structure, and the magnitude of ground motions used in pseudodynamic testing are not so severely limited as in shaking table tests. Consequently, pseudodynamic testing with larger scale models can provide useful data for the verification and improvement of current analytical methods.

3 From the difference between the pseudodynamic and shaking table test results, one can observe that the foundation stiffness of a test structure and the value of the structural period with respect to the frequency content of an earthquake record have a significant influence on the seismic response and the extent of structural damages developed. Consequently, these are important considerations in testing, design, and analysis of seismic-resistant structures, and several ground motions should be considered in design and analysis.

4 The capability of an offshore tower to resist an "aftershock" depends on its post-damage structural properties as well as on its energy-dissipation capacity.

5 The lateral load resistance and the hysteretic energy dissipation of the tubular X-braced frames were mainly contributed by the diagonal braces. The braces with smaller $D/t$ ratios had greater energy-dissipation efficiency and durability under cyclic loadings. A good understanding of the post-buckling strength of the braces is important in the inelastic design and analysis of braced structures. The results of these experiments provide useful information to develop and evaluate analytical brace models.

6 Based on the test results, a properly designed and constructed offshore structure can sustain intense seismic excitations and develop a significant energy-dissipation capacity. However, great uncertainties are associated with the determination of realistic environmental loadings (including seismic and wave actions) and structural boundary conditions (such as the soil-structure interaction). As mentioned in the foregoing, these could have significant influences on the dynamic response of a structure. Hence, further experimental and analytical studies are recommended to identify the exact

influence of the foregoing parameters on the inelastic performance of offshore structures.

7 The pseudodynamic method is one of the most promising experimental techniques for future studies. Hydrodynamic effects can be conveniently approximated in the pseudodynamic formulation by modifying the inertia and damping properties of a structure using appropriate inertia and drag coefficients, and by the determination of hydrodynamic loading from appropriate wave theories. The effects of soil-structure interaction can also be included using analytical substructures. Testing structures subjected to multiple components of excitations poses no analytical difficulties. Much research is to be done to increase the reliability of the method of testing complicated structural systems, and to extend the versatility of the technique.

## Acknowledgments

The financial support of the National Science Foundation in sponsoring the experimental research and the developmental work on the pseudodynamic method is gratefully acknowledged. The authors would like to thank S. Dermitzakis for his assistance in performing the tests, and C. Thewalt for developing the data reduction and computer graphics programs.

## References

1 American Petroleum Institute, "Recommended Practice for Planning, Designing, and Constructing Fixed Offshore Platforms," Dallas, Tex., 10th Edition, 1979.

2 Takanashi, K., et al., "Non-linear Earthquake Response Analysis of Structures by a Computer-Actuator On-line System," *Bulletin of Earthquake Resistant Structure Research Center*, Institute of Industrial Science, University of Tokyo, No. 8, 1975.

3 Takanashi, K., et al., "Inelastic Response of H-Shaped Columns to Two Dimensional Earthquake Motions," *Bulletin of Earthquake Resistant Structure Research Center*, Institute of Industrial Science, University of Tokyo, No. 13, Mar. 1980.

4 Okada, T., et al., "Nonlinear Earthquake Response of Equipment System Anchored on R/C Building Floor," *Bulletin of Earthquake Resistant Structure Research Center*, Institute of Industrial Science, University of Tokyo, No. 13, Mar. 1980.

5 McClamroch, N. H., Serakos, J., and Hanson, R. D., "Design and Analysis of the Pseudo-Dynamic Test Method," *UMEE* 81R3, University of Michigan, Ann Arbor, Sept. 1981.

6 Shing, P. B., and Mahin, S. A., "Experimental Error Propagation in Pseudodynamic Testing," *UCB/EERC-83/12*, Earthquake Engineering Research Center, University of California, Berkeley, June 1983.

7 Ghanaat, Y., and Clough, R. W., "Shaking Table Tests of A Tubular Steel Frame Model," *UCB/EERC-82/02*, Earthquake Engineering Research Center, University of California, Berkeley, Jan. 1982.

8 Zayas, V. A., Mahin, S. A., and Popov, E. P., "Cyclic Inelastic Behavior of Steel Offshore Structures," *UCB/EERC-80/27*, Earthquake Engineering Research Center, University of California, Berkeley, Aug. 1980.

9 Clough, R. W., and Penzien, J., *Dynamics of Structures*, McGraw-Hill, 1975.

10 Bathe, K., and Wilson, E. L., *Numerical Methods in Finite Element Analysis*, Prentice Hall, 1976.

11 Newmark, N. M., "A Method of Computation for Structural Dynamics," *Journal of the Engineering Mechanics Division*, ASCE, No. EM3, Vol. 85, July 1959.

12 Hanson, R. D., "Comparison of Static and Dynamic Hysteresis Curves," *Journal of the Engineering Mechanics Division*, ASCE, No. EM5, Vol. 92, Oct. 1966.